ANL-6733
Reactor Technology
(TID-4500, 30th Ed.)
AEC Research and
Development Report

ARGONNE NATIONAL LABORATORY
9700 South Cass Avenue
Argonne, Illinois 60440

A TWO-ZONE FAST CRITICAL EXPERIMENT
(ZPR-III Assembly 42)

by

P. I. Amundson, R. L. McVean,
and J. K. Long

Idaho Division

January 1964

Operated by The University of Chicago
under
Contract W-31-109-eng-38
with the
U. S. Atomic Energy Commission

DISCLAIMER

TABLE OF CONTENTS

LIST OF FIGURES

LIST OF FIGURES

LIST OF TABLES

A TWO-ZONE FAST CRITICAL EXPERIMENT
(ZPR-III Assembly 42)

by

P. I. Amundson, R. L. McVean, and J. K. Long

ABSTRACT

This study was conducted to determine what properties of a previously studied dilute power reactor could be duplicated in a smaller two-zone assembly. Reactivity measurements performed included determinations of plate-orientation worth, homogeneity corrections, reactor-segment worths, central reactivity coefficients, and radial worth distributions of axial columns of core materials. Spectral index determinations included: central fission ratios, nuclear track emulsion measurements, fission counter traverses, Rossi-alpha measurements, sodium activation, and natural and enriched uranium foil measurements.

INTRODUCTION

Exploratory work into two-zone systems is based on the inability of experimentalists to assemble mockups of very large fast power breeder reactors because the size is limited in present critical facilities.

The two-zone system was conceived to try to fit a portion of a very large power breeder reactor into an existing critical facility. A small, subcritical portion of a large dilute system is positioned in the center of the critical facility matrix and surrounded by enough high-enrichment driver material to make the system critical. If the driver diluents and a filter between the driver and core are chosen properly, the higher-energy driver flux can be modified enough to allow neutron equilibrium over a major portion of the dilute central area. Should this system prove workable, it may be possible to study some of the more interesting parameters of the large dilute systems, such as the sodium void coefficient vs. sodium fraction, clad composition, and core height for a series of very large reactors.

The primary purpose of the ZPR-III Assembly 42 was to determine how much meaningful information can be derived from the two-zone method To do this, the central core area of Assembly 42 was made an exact duplicate of a previously run dilute, simulated uranium carbide reactor

(Assembly 34).[1] The driver zone was chosen because it would imitate the conditions expected with future, larger two-zone systems. These conditions are: a driver spectrum harder than the central spectrum; a relatively high power density and reactivity density; a simple composition that would yield to analysis; and stainless steel and graphite used to temper the driver spectrum. The purpose of the filter which separates the two zones is to make gross shifts in the neutron-energy spectrum between the driver and core, so that as large as possible a region of the central zone will be useful for physics studies.

THE ZPR-III MACHINE

ZPR-III is a critical assembly divided into two separable halves that allow for loading safety and ease of loading from the radial midplane. In the separated (shutdown or loading) state the reactivity hazard is small.

The primary reactor feature allowing simple assembly design consists of a 31 x 31 array of horizontal stainless steel tubes, each having a cross-sectional area of 4.57 sq in. and a depth of 33.5 in. A view of the ZPR-III machine is given in Fig. 1. All control instrumentation is located

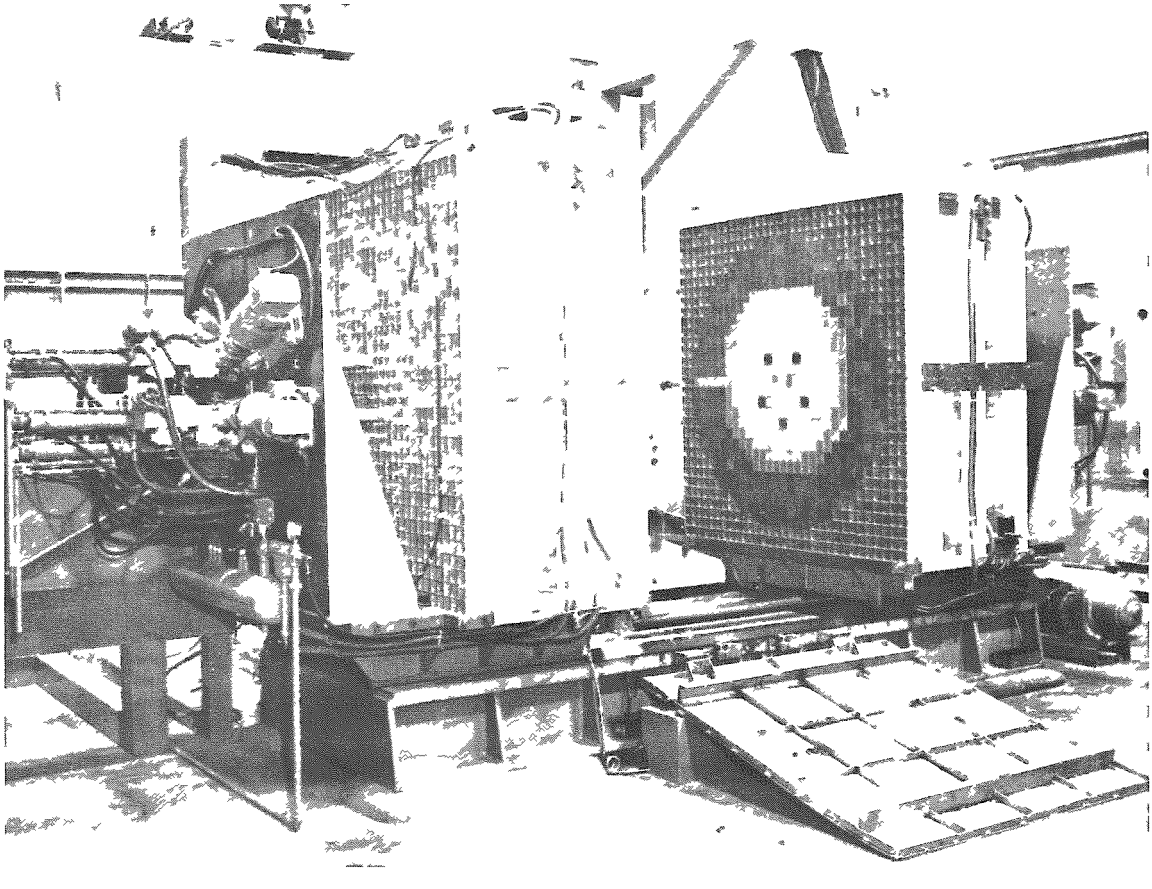

Fig. 1. View of ZPR-III

above the machine halves. Safety-control rods which feature electrical drive and pneumatic scram power are inserted from the axial ends of the reactor (five safety control rods enter each half).

Assemblies are constructed by preloading perforated stainless steel drawers with the normally prescribed composition of $\frac{1}{8}$-in.-thick plates of fuel and diluent materials (see Fig. 2). These core drawers are inserted into the matrices of each half in a repetitive pattern until criticality can be achieved with the halves together and all control-safety rods inserted. A more complete description of the ZPR-III facility has been given by Cerutti et al.[2]

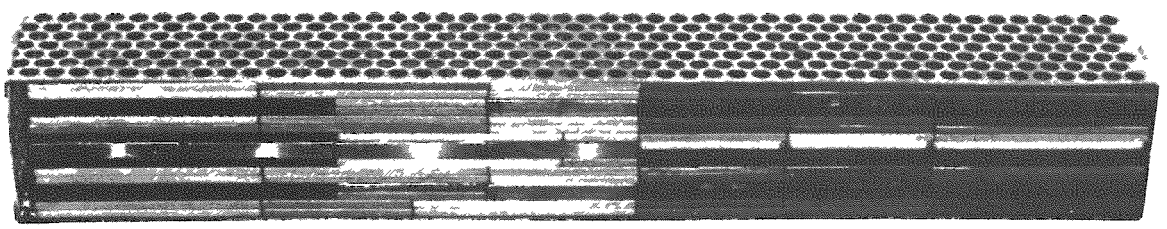

Fig. 2. Typical Drawer Structure

PHYSICAL DESCRIPTION OF ASSEMBLY

Assembly 42 is a two-zone cylindrical reactor that consists of two fuel zones separated by a filter of depleted uranium. The two zones are completely blanketed both axially and radially with depleted uranium.

A face view of one-half of the assembly is shown in Fig. 3. For safety purposes, the assembly is positioned in the ZPR-III matrix with the cylinder lying on its side. This procedure is normally followed in ZPR-III so that insertion of the fuel-containing control-safety rods will result in reactivity changes that are predictable and nonhazardous. In Assembly 42 control-safety rod travel is limited to movement through the axial blanket into the zone for which a specific control-safety rod is designed.

The central zone (core area) is 34.06 in. in length and has an effective radius of 9.22 in. Each drawer in this zone contains one column of enriched uranium, two columns of graphite, two columns of depleted uranium, three columns of stainless steel, two columns of 100% aluminum, two columns of 63% reduced-density aluminum, and four columns of 45% reduced-density aluminum. The core area drawer column arrangement is shown in Fig. 4. This arrangement is a duplicate of that of Assembly 34.

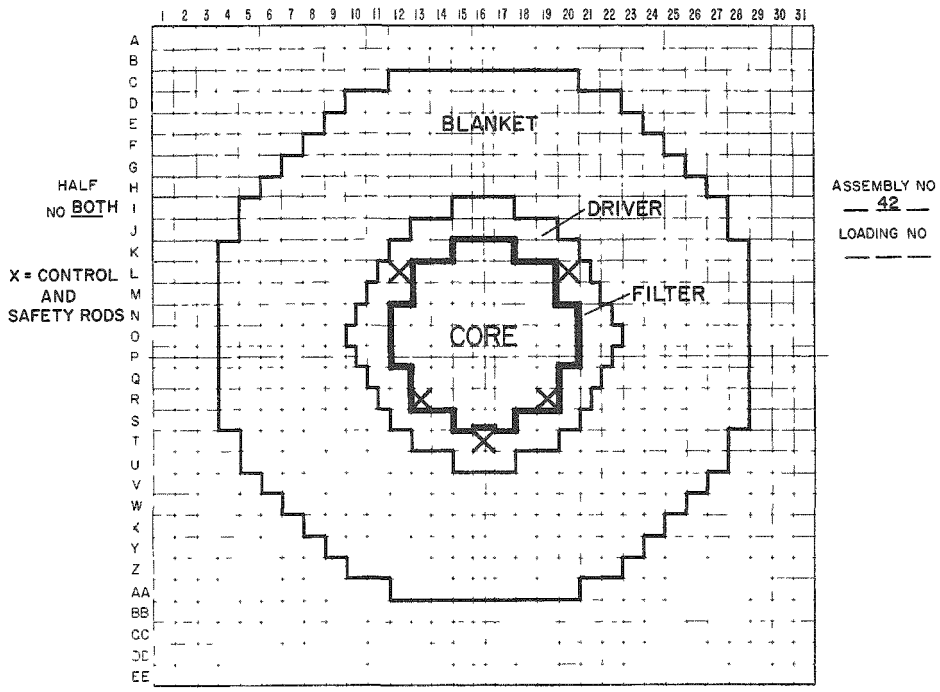

Fig. 3. Face View of One-half Assembly

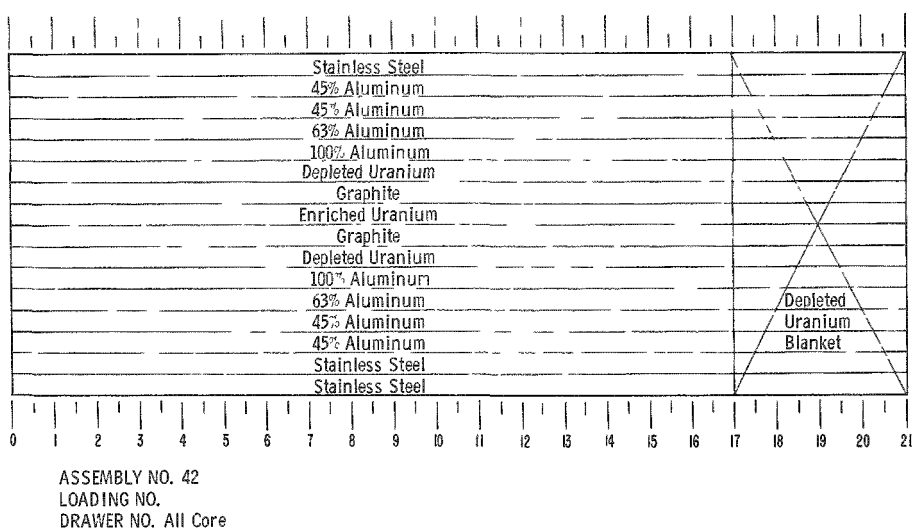

Fig. 4

Core Area Drawer Loading

The radial periphery of the core zone is surrounded by a nominal $\frac{1}{2}$-in.-thick depleted uranium filter. The filter has the same axial length as does the core zone. Although the mass of depleted uranium in the filter would indicate a radial dimension slightly in excess of $\frac{1}{2}$ in. in thickness with an inner radius of 9.22 in., the filter zone is actually 0.71 in. in radius due to the volume taken up by the stainless steel in the matrix and perforated drawers, and inherent construction voids characteristic of all drawer loadings.

Surrounding the filter zone radially and with an axial length equal to it is a driver zone containing approximately twice the U^{235} volume fraction of the core. The driver zone has an effective inner radius of 9.93 in. and an effective outer radius of 13.11 in. Each full drawer in the driver zone contains 2 columns of enriched uranium, one column of depleted uranium, 9 columns of graphite, and 4 columns of stainless steel. The material arrangement in a typical driver drawer is given in Fig. 5. All half drawers in the driver contain the same material arrangements as a full drawer up to the point in the drawer where blanket material starts. A portion of the driver drawers above and below the filter have the columns of material in a horizontal plane as shown in Fig. 6. This arrangement of material was necessitated for some of the 3/4 drawers because of the lack of small-sized pieces of various materials necessary to make a 3/4 drawer with columns in the vertical plane.

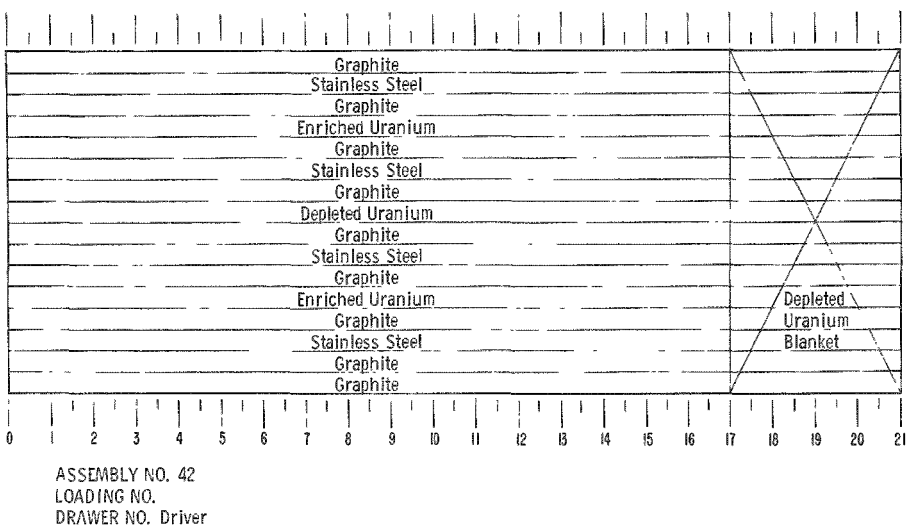

Fig. 5
Top View of General Driver Drawer Loading

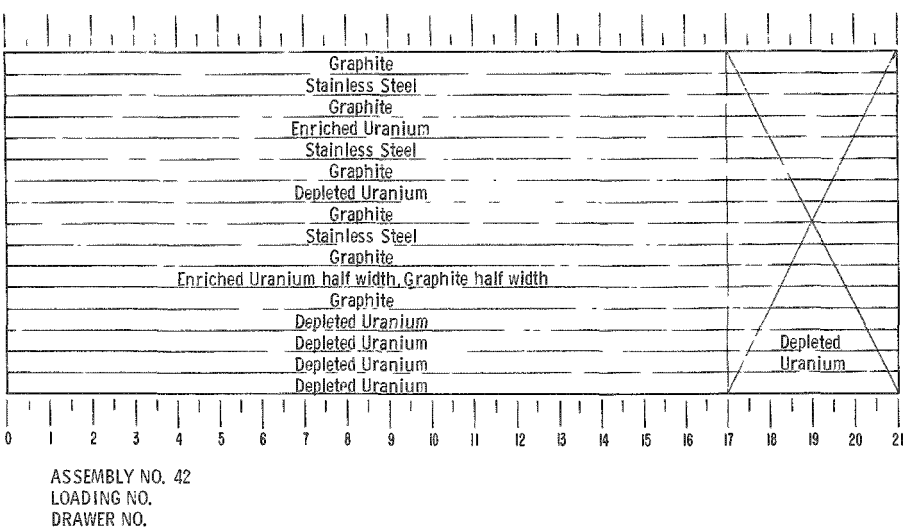

Fig. 6. Arrangement of Driver Drawers (Horizontal Plates) of Fig. 3

The compositions of the various zones are given in Table I. Although the core drawer arrangements are the same as in Assembly 34, the volume fractions differ slightly because the filter cuts into portions of the edge of the core; also, the ratio of the control-safety drawer stainless mass is different from the total core mass.

Table I

REACTOR CONSTANTS

Volume % (g cc)	Core	Filter	Driver	Blanket			
				Radial Inner	Radial Outer	Axial	Total
U^{235} (18.75)	5.04	0.17	9.29	0.17	0.17	0.17	0.17
U^{238} (19.0)	11.0	80.1	6.54	83.5	83.1	82.3	83.2
Stainless Steel (7.85)	22.6	6.9	28.6	9.1	7.3	9.3	8.2
Graphite (1.43)	12.5	-	51.3	-	-	-	-
Aluminum (2.7)	25.6	-	-	-	-	0.02	-
Volume (liters)	149.12	25.8	157.20	698.2	993.8	201.1	1893.1
Outer Radius (cm)	25.4	25.2	35.8	51.9	70.2	33.3	70.2
Length (cm)	86.5	86.5	86.5	142.4	142.4	= 55.9	142.4

The complete reactor, including the filter and blanket, is 56.06 in. long, has an effective radius of 27.63 in., and a volume of 134,440 $in.^3$ (2,203 liters).

APPROACH TO CRITICAL

On the basis of experience gathered while conducting the experimental program of Assembly 34, the initial loading contained the full expected core zone for Assembly 42. Since Assembly 34 was critical with over 500 kg U^{235}, a loading containing the same ratio of fuel to diluents and 141 kg U^{235} would be far subcritical. This subcritical core was completely blanketed both radially and axially with depleted uranium to a distance expected for the critical reactor, including a surrounding 12-in. blanket.[3]

The approach to critical consisted of stepwise radial replacements of blanket drawers with drawers containing the materials constituting the driver zone. After each incremental addition of driver material, the halves were brought together and the degree of subcriticality estimated as based on the inverse of the neutron count rate from two proportional counters situated at the axial core-blanket interface in drawers 1 and 2-O-14. The counters were positioned to minimize nonlinearities in the critical-approach curve, that is, the plot of inverse count rate vs. mass of U^{235} (see Fig. 7).

After reaching criticality, control rod No. 10 was calibrated by measuring the stable period associated with each incremental change in control rod position. By alternately adjusting two control rods in opposite directions and by assuming that the control rods have no interaction, a calibration

over several inches of rod No. 10 was made. This control rod, located in the driver region, indicated a worth of approximately 80 Ih with a differential worth near the center of the rod of approximately 9 Ih/in. The calibration curve for rod No. 10 is given in Fig. 8. The reactivity-period curve used is reproduced in Fig. 9.

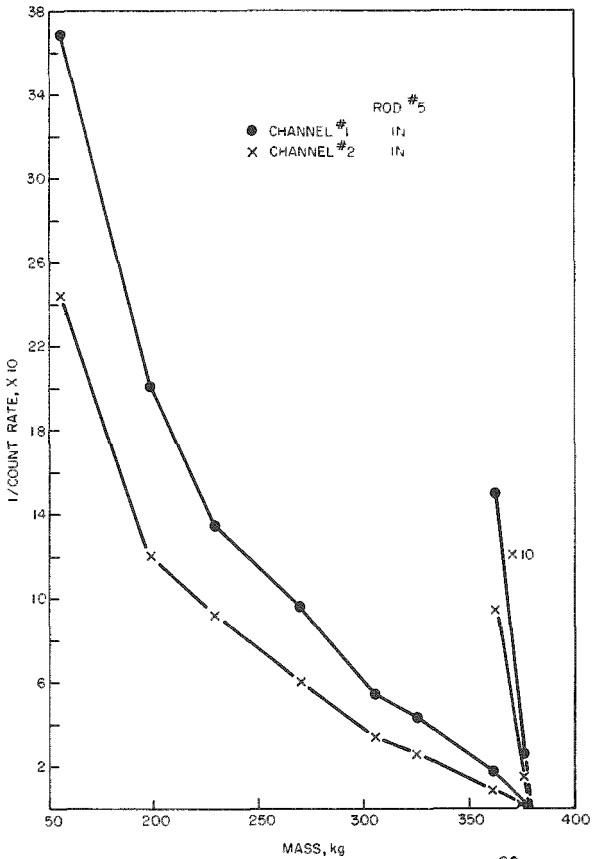

Fig. 7

Critical Approach

The reactivity worth of core material substituted for blanket material at the edge of the driver was measured as a function of the change in critical rod position. After substitution of half-drawers at certain locations to round off the shape of the cylindrical reactor, the edge worth of driver material was measured as 25 Ih/kg U^{235}. This worth, along with the control rod calibration, was used to calculate an exact critical mass of 379.4 kg U^{235}, exclusive of the 0.7 kg U^{235} in the filter.

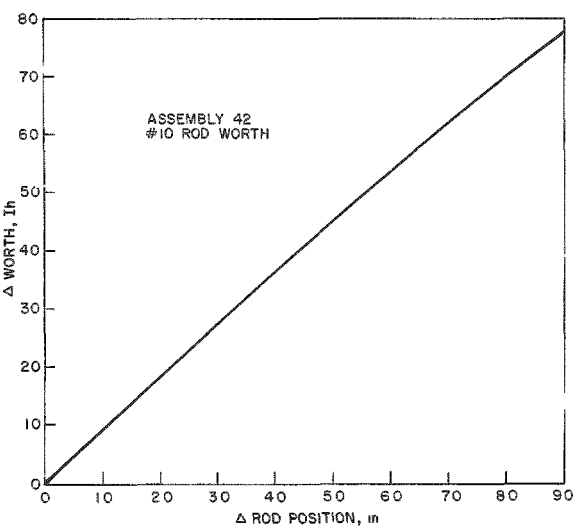

Fig. 8. Control Rod Calibration

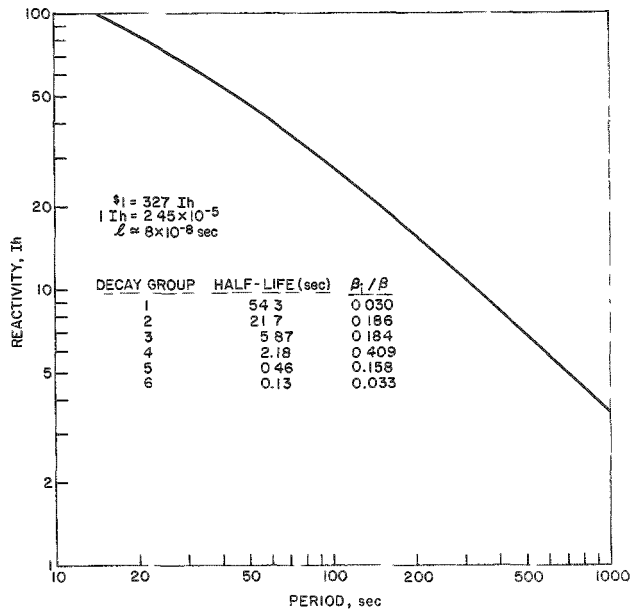

Fig. 9

Reactivity Period Curve

PLATE ORIENTATION EXPERIMENTS

Some concern has been expressed about the effects of plate orientation in regions where the flux gradient is steep. In order to clarify the existence of reactivity changes due to these effects and to measure these effects semiquantitatively if possible, two experiments were conducted.

To check for possible effects on reactivity of core plate orientation in core material near the driver, the fuel plates in drawers 1 and 2, L-14 and 18, and 1 and 2, R-14 and 18 (see Fig. 10) were oriented 90°

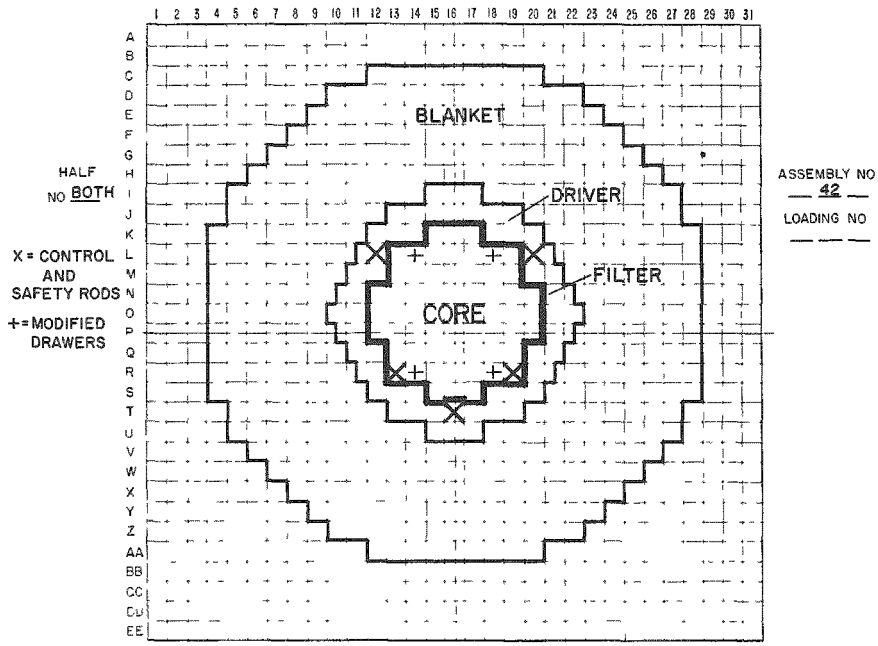

Fig. 10

Core Fuel Plate Reorientation

to make the fuel plates parallel to the filter material in this region. The orientation process involved keeping the plates in positions that resulted in the same average center of mass for each drawer regardless of orientation of fuel plates. This process would eliminate the possibility of any net radial shifting of fuel if the gradient in the vicinity was linear.

The resulting reactivity change was 1.26 Ih for an orientation of 9.2 kg of enriched uranium at an average radius of 6.17 in.

The second experiment consisted of orienting the columns of enriched uranium in the driver at a radius such that the gradient would be steep. The fuel columns in drawers 1 and 2, I-15, 16, and 17, and 1 and 2, U-15, 16, and 17 (see Fig. 11) were oriented 90°, resulting in a reactivity change of 2.36 Ih for 27.6 kg U^{235} at an average radius of 13.23 in.

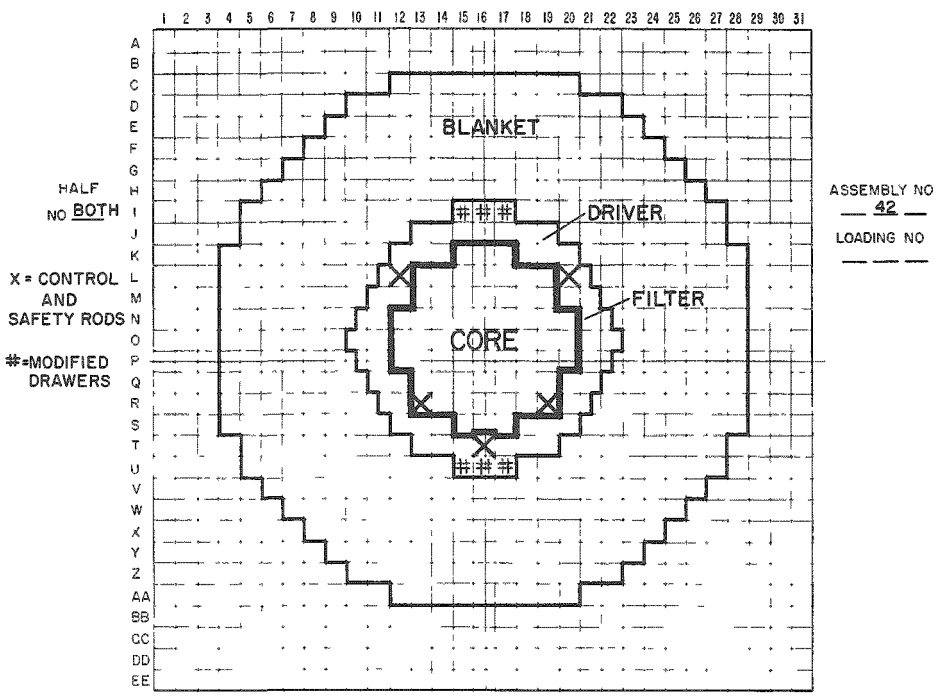

Fig. 11. Driver Fuel Plate Reorientation

Although the results indicated a small negative change in the core at R = 6.17 in., and a slightly larger positive change in the driver at R = 13.23 in., no conclusions have been drawn since the evaluation does not take into account the possible effects of large nonlinear gradients resulting in net effective shifts of fuel nor does the error due to closure of the halves of $\pm\frac{1}{2}$ Ih allow any degree of confidence in the accuracy of either experiment.

HETEROGENEITY FUEL-BUNCHING EXPERIMENTS

Because of problems associated with orientation of fuel in the core and driver and the limited number of enriched uranium pieces of certain required specific sizes, the heterogeneity experiments for the core and driver had to be conducted separately. It was assumed that since heterogeneity corrections are functions of local perturbations, there will be no gross interaction between the core and driver during the associated bunching experiments.[4] This allows a simple summing of the effects in each zone to arrive at an overall homogeneity correction for the entire reactor. Ten drawers of a representative segment of each half of the core zone (see Fig. 12) were alternately bunched and unbunched.

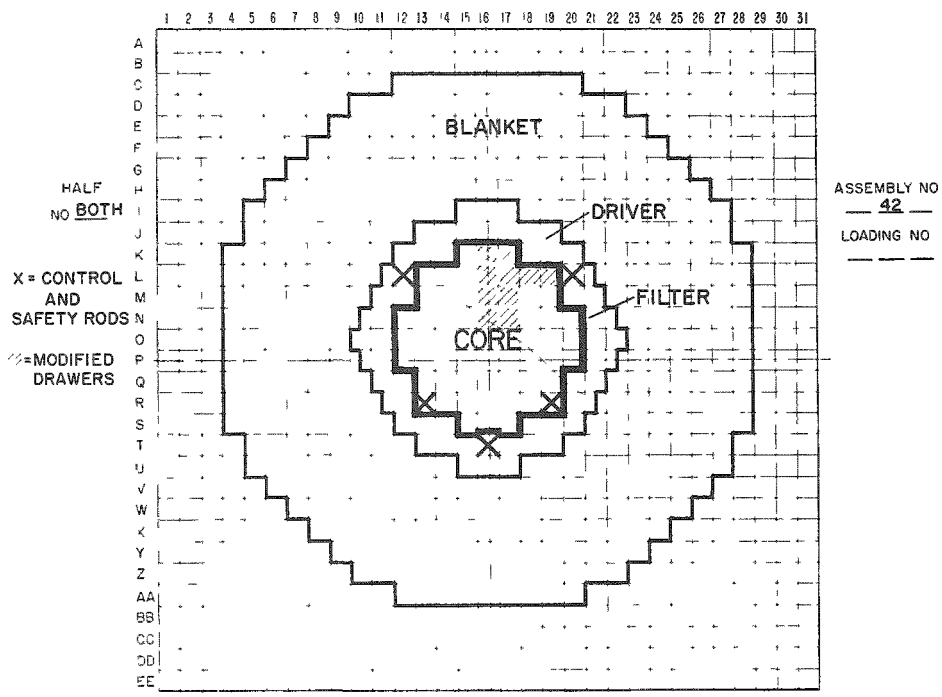

Fig. 12. Core Homogeneity Experiment

The 20 drawers containing 23.1 kg U^{235} when bunched (see Fig. 13) resulted in an increase in reactivity of 31.65 Ih. Bunching of the entire 141 kg U^{235} in the core would thus result in a gain of 193 Ih.

The same 20 drawers were used to determine the effect of changing the thickness of the fuel columns from $\frac{1}{8}$ to $\frac{1}{16}$ in. Unbunching the $\frac{1}{8}$-in. columns in these 20 drawers to $\frac{1}{16}$-in. columns (see Fig. 14) involved 23.14 kg U^{235}, resulting in a loss of 20 Ih. If the entire core zone had been unbunched in this manner, the associated loss in reactivity would have been 121.8 Ih.

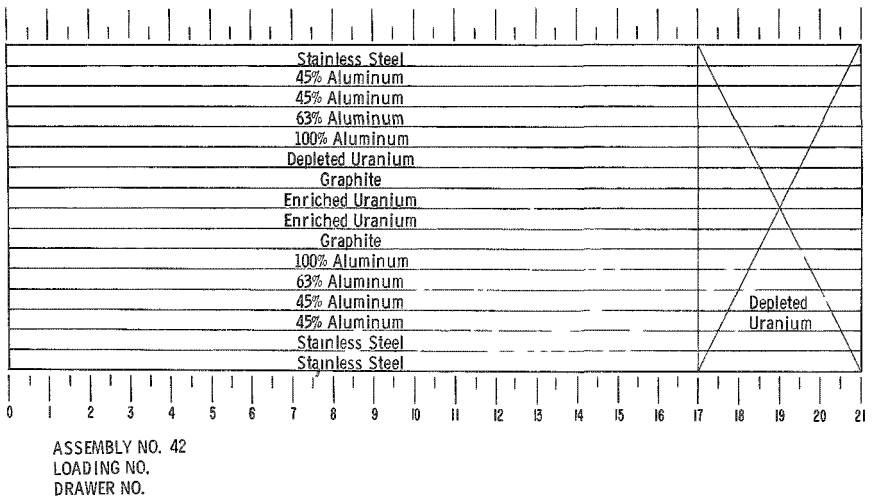

Fig. 13

Core Bunching Arrangement (for reference see Fig. 4)

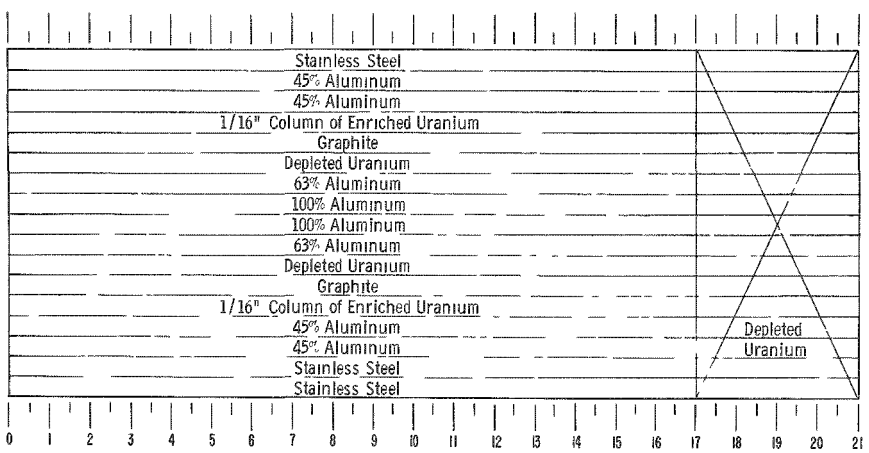

Fig. 14

Core Unbunching Arrangement

Four full drawers and two half drawers (see Fig. 15) in each half were used as a representative segment for bunching and unbunching the

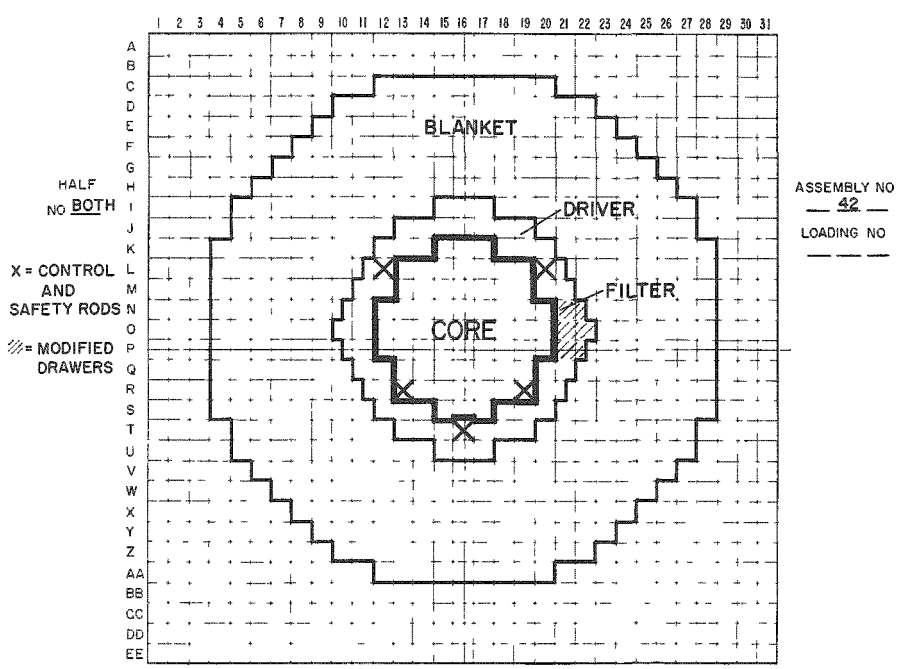

Fig. 15

Driver Homogeneity Experiment

driver zone. The driver bunching (see Fig. 16) experiment with 23.1 kg U^{235} resulted in a gain of 15.3 Ih. Extrapolation to the full 239-kg driver would result in a reactivity gain of 158 Ih.

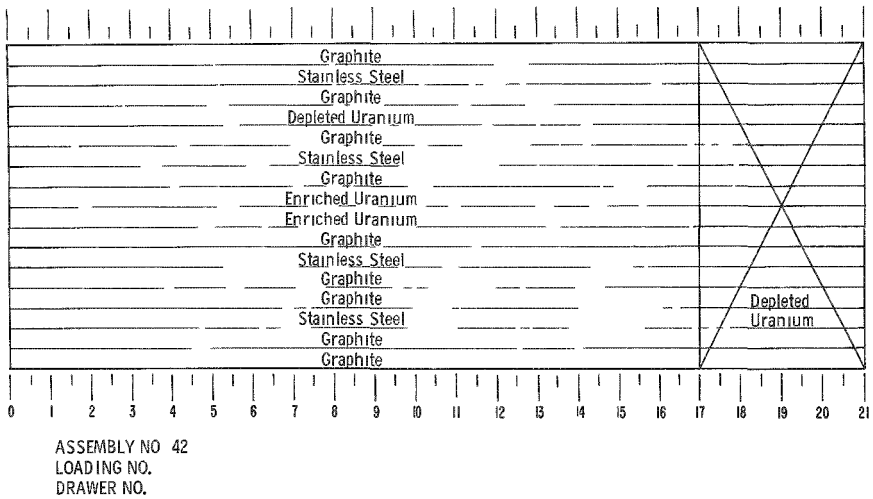

Fig. 16

Driver Bunching Arrangement (for reference see Fig. 5)

This same segment, now containing 23.14 kg U^{235} when unbunched (see Fig. 17) from $\frac{1}{8}$- to $\frac{1}{16}$-in.-thick columns, resulted in a loss in reactivity of 4.3 Ih. Extrapolation to a completely unbunched driver results in a loss of 44.6 Ih.

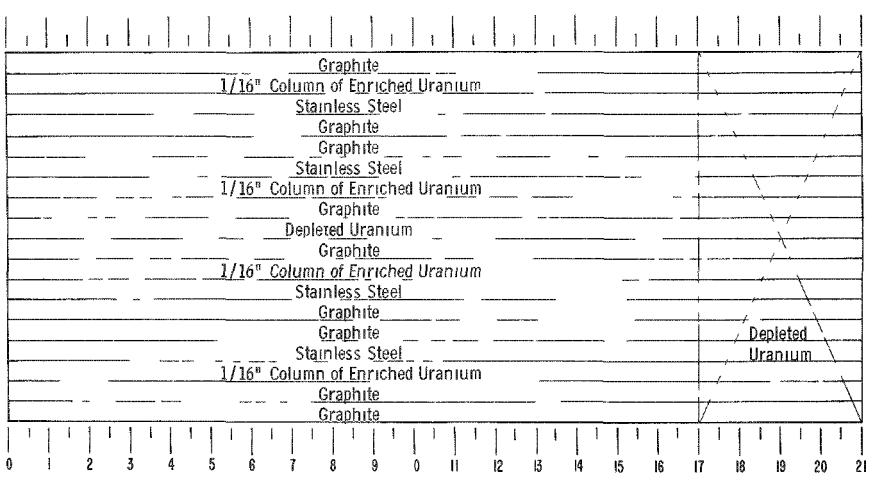

Fig. 17. Driver Unbunching Arrangement (for reference see Fig. 5)

The results of the bunching experiments are shown in Fig. 18, where relative reactivity is given as a function of fuel thickness and includes an extrapolation to zero thickness. Summation of the zero fuel-thickness values for both core and driver would result in considerably less than the nominal 450 Ih which can be taken as an average correction (approximately 1%; 0.7-1.5%) for most recent large dilute assemblies.(5)

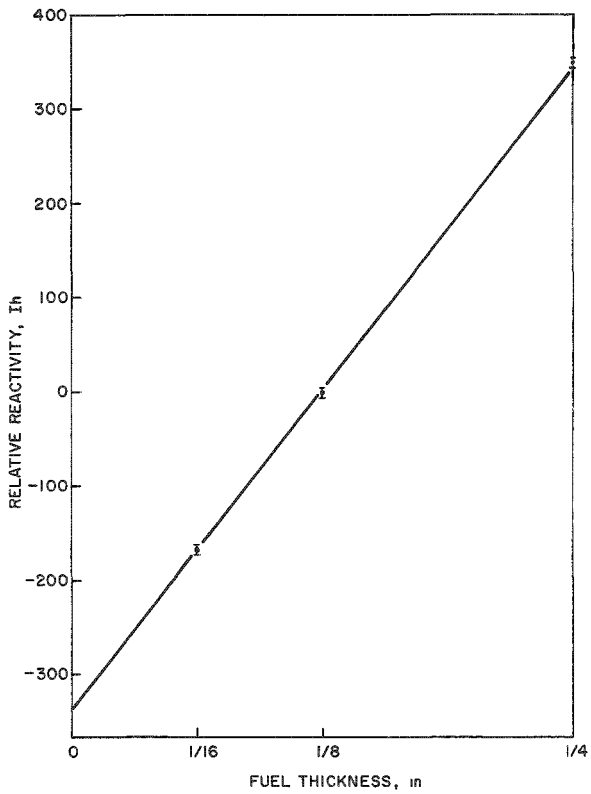

Fig. 18

Homogeneity Correction

WORTH OF CORE DRAWERS AT VARIOUS RADIAL POSITIONS

The reactivity worths of core drawers at three different radial positions were measured, relative to void, by the technique of subcritical multiplication determination. This technique involves removing a core drawer, thus causing the reactor to be subcritical with the halves together and all rods inserted. A calibrated control rod is then moved to 2 or 3 different positions with two separate BF_3 counters measuring the subcritical count rates at each control rod position. The reciprocal count rate is then used to extrapolate to critical and the control rod calibration used to determine the degree of subcriticality. This reactivity is then added to the known excess of the reference core to determine the worth of the removed drawer. The results of these measurements are given in Table II.

Table II

MEASUREMENTS OF DRAWER WORTHS

Radius (in., cm)	Drawer Matrix Position	Worth (Ih)	Comments
0,0	2 O 16	107 ± 5	Center of Core (Fig. 4)
8.71, 22.1	2 K 16	84 ± 4	Core, Outer Edge (Fig. 4)
10.9, 27.7	2 O 21	130 ± 6	Driver, Inner Edge (Fig. 5)

CENTRAL REACTIVITY MEASUREMENTS

Measurements were made of the reactivity change due to the insertion of various materials at the core center. All the fissile materials (U^{235}, U^{233}, and Pu^{239}) in these measurements were approximately $2 \times 2 \times \frac{1}{4}$ in. in size. The U^{235} sample was in the form of two $\frac{1}{8}$-in.-thick plates, and the plutonium and U^{233} samples were canned in aluminum. The reference loadings for the small fissile samples contained one crosswise column of 45% aluminum and one of 63% aluminum in the first quarter-inch of two opposing central drawers. The fissile materials were substituted either clad in (in the case of plutonium and U^{233}) or sandwiched between (in the case of U^{235}) 100% aluminum such that the net aluminum change was negligible.

To measure the central reactivity worths of nonfissile materials (depleted uranium and thorium), a special set of two drawers was used. The perforated front sections of these drawers were recessed one inch into the drawer. By use of these drawers in opposing central matrix tubes, an 8-cu in. void was created at the core center. The changes in reactivity were measured for 2 x 2 x 1-in. samples inserted in these spaces, except for the materials silver and boron carbide, for which a single 1 x 2 x 2-in. sample and a 1 x 2 x $\frac{1}{4}$-in. sample were used, respectively.

The reactivity changes measured were taken as the difference in the calibrated control rod position for the changed core over that for the reference core for each sample. For large changes in reactivity, the associated reactivities in inhours for each control rod position were read directly from the control rod calibration curve. For small changes in reactivity, to obtain the greatest accuracy, the differential calibration over a linear portion of the control rod was used.

The reactivity worths of the materials examined are given in Table III. The errors cited are based on an estimated ± 0.5 Ih for half-closure reproducibility.

A perturbation theory code written by A. Hess, programmed for the IBM 1620, was used to calculate some of the central material worths.[6] The results are given in Table III.

Table III

CENTRAL REACTIVITY COEFFICIENTS

[All values in mb/atom, normalized to $(\nu-1)\sigma_f-\sigma_c$ for Pu^{239}]

Material	Assembly 34			Assembly 42		
	Experimental (1h/kg)	Calc (mb/atom)	Measured (mb/atom)	Experimental (1h/kg)	Calc (mb/atom)	Measured (mb/atom)
			Using Cross-section Set 635[5]			
U^{235}[b]	107 ± 2.0	1910	1990 ± 35	117 ± 2.0	1916	2010 ± 35
Pu^{239}[b]	182 ± 2.5	3404	3404 ± 40	197 ± 2.5	3402	3402 ± 40
U^{233}[b]	206 ± 2.5	3630	3700 ± 40	223 ± 2.5	3636	3860 ± 40
U^{238}[b]	-5.8 ± 0.3	-105	-108 ± 5	-8.0 ± 0.3	-105	-108 ± 5
Thorium	-12.7 ± 0.3	-240	-230 ± 6	-13.0 ± 0.3	-240	-217 ± 6
Zirconium	-1.2 ± 0.5	-13	-8 ± 3	-1.3 ± 0.5	-14	-9 ± 3
Sodium[a]	7.2 ± 5.0	10	13 ± 9	10.3 ± 5.0	8	17 ± 9
Lead	-0.09 ± 0.3		-1 ± 4	-0.3 ± 0.3		-4 ± 4
Carbon	36.6 ± 2.5	21	34 ± 3	35.5 ± 2.5	19	31 ± 3
Bismuth	-0.4 ± 0.5		-6 ± 9	-0.07 ± 0.4		-1 ± 9
Aluminum	0.94 ± 0.5	4	2 ± 1	0.2 ± 0.5	3	0.4 ± 1
Ph-I Oxide[a,d]	-14.8 ± 2.5		-164 ± 30	-15.3 ± 2.5		-157 ± 30
Ph-II Oxide[a,d]	-13.4 ± 2.5		-141 ± 30	-14.5 ± 2.5		-142 ± 30
Niobium[a]	-16.0 ± 1.0	-129	-116 ± 8	-16.6 ± 1.0	-128	-111 ± 8
Molybdenum	-9.5 ± 0.5	-77	-71 ± 4	-10.3 ± 0.5	-79	-71 ± 4
Mercury[a]	-5.0 ± 0.5		-78 ± 8	-5.4 ± 0.5		-78 ± 8
Al_2O_3	8.1 ± 1.5			8.3 ± 1.5		
Oxygen[e]		15	21 ± 8		14	20 ± 8
Lithium[a]	-81.8 ± 10.0		-44 ± 5	-97.6 ± 10.0		-41 ± 5
Beryllium	84.8 ± 2.0		59 ± 1	83.1 ± 2.0		54 ± 1
B^{10}[c]	-2060 ± 50	-1450	-1610 ± 40	-2290 ± 50.0	-1410	-1650 ± 40
Tantalum[a]	-28.7 ± 0.5	-358	-400 ± 10	-30.2 ± 0.5	-354	-394 ± 10
SS	-1.5 ± 0.5	-7	-6 ± 2	-1.7 ± 0.5	-9	-7 ± 2
Silver	-44.2 ± 0.4		-370 ± 5	-50.4 ± 0.8		-393 ± 10
			Using Cross-section Set 145[7]			
Nickel	-2.4 ± 0.5	-9	-11 ± 2	-2.5 + 0.5	-10	-11 ± 2
Chromium[a]	-0.6 ± 1.0	-10	-2 ± 3	-0.7 ± 1.0	-11	-3 ± 3
SS	-1.5 ± 0.5	-6	-6 ± 2	-1.7 ± 0.5	-8	-7 ± 2

[a] Corrected for reactivity effects of stainless steel canning material.
[b] Corrected for effects of all other isotopes contained in samples.
[c] Corrected for effects of B^{11} and carbon in enriched B_4C sample.
[d] Physicum samples fully described in reference 8.
[e] Oxygen worth calculated from Al_2O_3 measurement.

REACTIVITY WORTHS OF AXIAL COLUMNS OF REACTOR MATERIALS AT VARIOUS RADII

To obtain a distribution of the reactivity worths of reactor materials at various radii that would be amenable to calculation, measurements were made of the reactivity changes associated with substitution of full axial columns of various materials at three different radii in the core and one in the driver.

For aluminum, graphite, stainless steel, and depleted uranium in the core a drawer configuration shown in Fig. 19(a) was utilized. For these materials in the driver the drawer configuration of Fig. 19(b) was utilized.

The reactivity measurements were performed by initially determining the critical rod position for full-density aluminum in the sample columns, and then for 45% aluminum in these same columns. The worth of aluminum was then determined from the difference in critical rod position between the two runs and the mass change of aluminum between the two runs. The worth of aluminum was then used to calculate the reactivity of a reference core having these sample columns voided. This reference core was then used as a basis for determining the worths of columns of graphite, stainless steel, and depleted uranium.

The column worth of enriched uranium in the core was determined by replacing one $\frac{1}{8}$-in.-thick column of 100% aluminum. The drawer configuration for these measurements is shown in Fig. 19(c). In these measurements, the $\frac{1}{16}$-in. column of aluminum was used as a filler to keep the $\frac{1}{16}$-in. column of uranium in a specific position. The reactivity effects associated with the presence of this extra $\frac{1}{16}$-in. column of aluminum were accounted for in the calculation of the worth of the enriched uranium column.

The column worth of enriched uranium in the driver was determined by replacing a column of depleted uranium with a $\frac{1}{16}$-in. column of enriched uranium and a $\frac{1}{16}$-in. column of 100% aluminum [see Fig. 19(d)]. The reactivity effects associated with the withdrawal of the depleted uranium column and the addition of the $\frac{1}{16}$-in. aluminum column were accounted for in the calculation of the worth of the $\frac{1}{16}$-in. column of enriched uranium.

The results of these experiments are given in Table IV. From the column worth measurements of enriched and depleted uranium, worths for pure columns of U^{235} and U^{238} have been calculated and are given at the bottom of the table. In making corrections to determine the U^{235} and U^{238} column worth, the assumption was made that the reactivity effect per atom was the same for either specific isotope whether the isotope was contained in enriched or depleted uranium. Although this assumption is not necessarily valid, any error associated with it will be small compared with the reactivity measurement error due to closure of the halves.

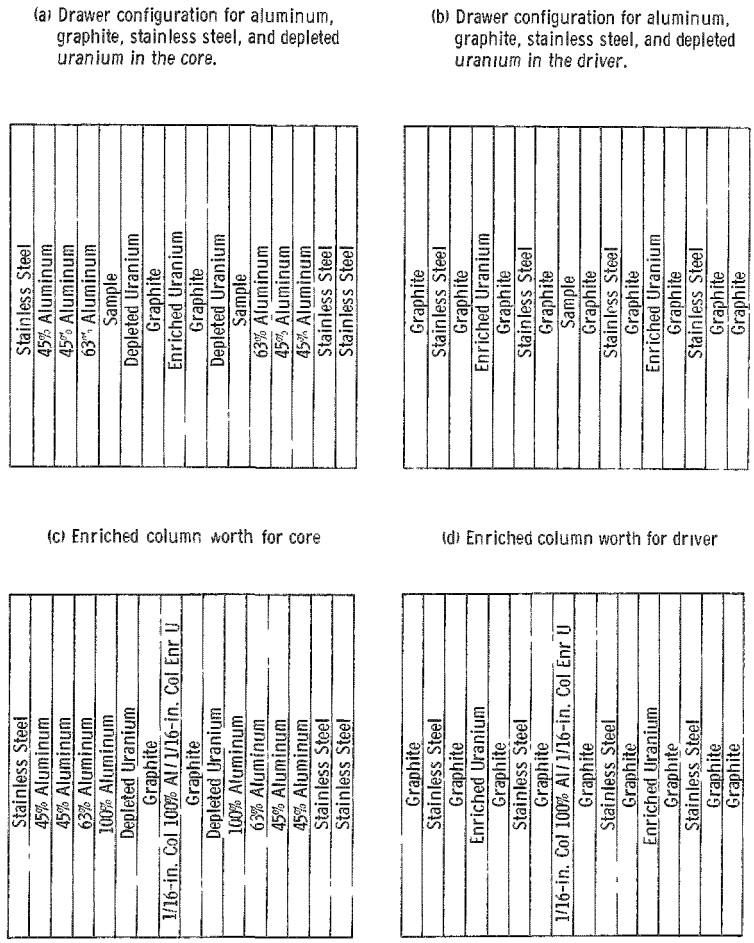

Fig. 19. Drawer Arrangement for Column Worth Measurement

Table IV

COLUMN WORTH (lh kg) MEASUREMENTS

Material	Radius			
	0 in. Core	4.88 in. (12.4 cm) Core	6.9 in. (17.5 cm) Core	11.75 in. (29.8 cm) Driver
Enriched Uranium	73.5 ± 0.9	72.5 ± 0.9	67.0 ± 0.9	36.9 ± 0.9
Depleted Uranium	-2.53 ± 0.09	-2.35 ± 0.05	-2.08 ± 0.05	0.40 ± 0.02
Stainless Steel	0.12 ± 0.12	0.45 ± 0.03	0.43 ± 0.03	2.60 ± 0.06
Aluminum	3.5 ± 0.3	3.7 ± 0.2	3.7 ± 0.2	6.6 ± 0.3
Graphite	29.4 ± 1.1	27.4 ± 0.3	23.8 ± 0.6	25.1 ± 0.6
U^{235}	79.0 ± 0.9	78.0 ± 0.9	72.0 ± 0.9	39.7 ± 0.9
U^{238}	-2.68 ± 0.09	-2.49 ± 0.05	-2.20 ± 0.05	-0.42 ± 0.02

The drawer positions used in these experiments are given in Fig. 20. Since the gradient in the core zone is not particularly steep, the quoted effective radii of the measurements in this zone are probably quite accurate. The effective radii quoted for the driver was taken as the physical center of the drawer and consequently may be in error due to a steep nonlinear flux gradient in this zone. Since the second derivative of the radial flux shape will be negative over most of the driver (the flux shape is convex), the effective center may be at a radius somewhat larger than 11.75 in.

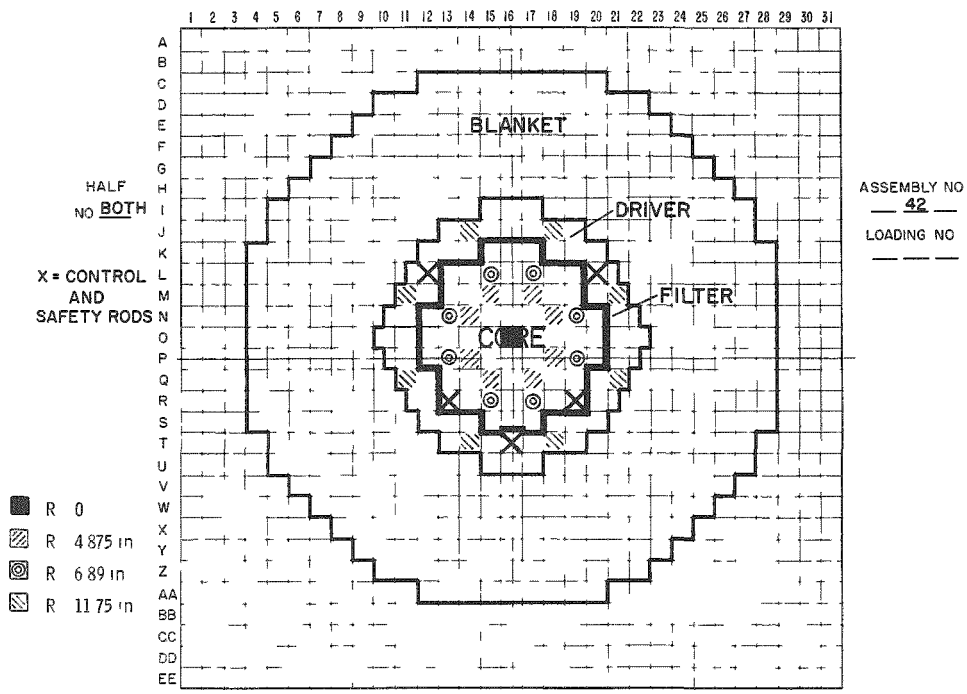

Fig. 20. Positions for Column Worth Measurements

REACTIVITY MEASUREMENT ERRORS

1. Error Associated with the Closure of the Halves

Based on experience gained over several years of operating ZPR-III, a half closure error of ±0.5 Ih has been accepted as an average figure, although smaller numbers (of the order of ±0.35 Ih), have been recorded for a limited number of experiments on specific large assemblies. The previous value has been taken as appropriate for measurements on this assembly.

2. Temperature Changes

Although the temperature coefficient of this assembly was not measured, experience with a large number of assemblies indicates a reactivity temperature coefficient of -1.5 Ih/°C. Since temperature changes within

the core are relatively slow, this error is unimportant and is corrected in all cases where temperature changes between runs were noticed. To avoid temperature corrections for runs involving only small changes in reactivity, measurements of this type were made previous to, or following, the specific reference.

3. Control Rod Movement and Backlash

The lower limit of reactivity change measurable due to required movement of the control rods is reported as ±0.04 Ih (or 10^{-6} $\Delta k/k$).(9) This error is very small compared with the half closure error and can be ignored for reactivity measurements associated with this assembly.

Thus, for practical purposes, the limitation of measurement of reactivity changes in Assembly 42 is associated mainly with half closure error (item 1). This inherent error (±0.5 Ih) is the basis for all reactivity measurement error limits quoted in this report.

FISSION RATIOS

Fission ratios of various fissile materials to U^{235} were measured at the core center with fission chambers of a parallel plate-type construction.(10) Precise construction techniques and the reported accuracy of the mass of the contained fissile material (±1%) make accurate measurements of effective cross-section ratios possible.

Two opposing central drawers (1 and 2-O-16) were reloaded to allow for positioning of a counter at the front of each drawer (see Fig. 21). A U^{235} counter (No. 5), used as a standard in flux monitoring, was placed in the

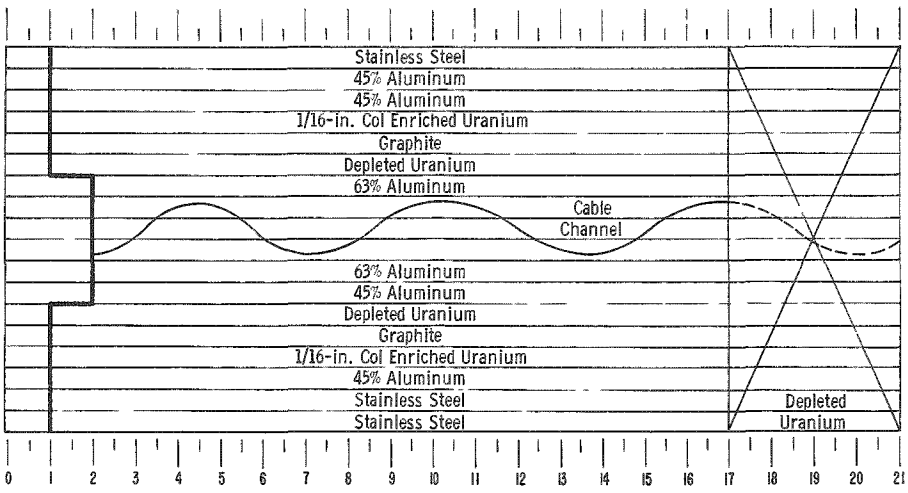

Fig. 21. Drawer Arrangement for Central Fission Ratio Measurements

front of one of the central drawers and maintained there throughout this experiment. The other counters were placed, one at a time, at the front of the opposing drawer. With the assembly at constant power the count rate of both the standard U^{235} counter and the adjacent fission counter were taken.

To correct for power variations between different runs, the count-rate data from the experimental fission counter were normalized to the count rate from the standard U^{235} counter. A set of simultaneous linear equations programmed for the IBM 1620 computer was used to correct for isotopic content of the counters used. The experimental fission ratios are given in Table V along with calculated ratios from the DSN spectrum using cross-section Set 635[11] and from a one-dimension cylindrical diffusion-theory calculation using cross-section Set 192.[12] Also listed are the fission ratios, both experimental and calculated, for Assembly 34. The central spectra resulting from Set 192 are given in Table VI.

Table V

CENTRAL FISSION RATIOS

Ratios	Calculated		Assembly 34		Assembly 42		
	Diffusion Theory	DSN	Measured	Corrected[11,13] for σ_{in}	Calculated Diffusion Theory	Measured	Corrected for σ_{in}
$\frac{\bar{\sigma}_f\ U^{238}}{\bar{\sigma}_f\ U^{235}}$	0.039	0.0407	0.034	0.037	0.039	0.034	0.037
$\frac{\bar{\sigma}_f\ U^{236}}{\bar{\sigma}_f\ U^{235}}$	0.091	0.0949	0.080	0.085	0.091	0.079	0.084
$\frac{\bar{\sigma}_f\ U^{234}}{\bar{\sigma}_f\ U^{235}}$	0.287	0.303	0.247	0.257	0.287	0.252	0.262
$\frac{\bar{\sigma}_f\ Pu^{240}}{\bar{\sigma}_f\ U^{235}}$	0.296	0.3111	0.271	0.282	0.296	0.282	0.293
$\frac{\bar{\sigma}_f\ Pu^{239}}{\bar{\sigma}_f\ U^{235}}$	1.13	1.153	1.07	1.07	1.13	1.08	1.08
$\frac{\bar{\sigma}_f\ U^{233}}{\bar{\sigma}_f\ U^{235}}$	1.54	1.545	1.45	1.45	1.54	1.43	1.43

Table VI

CALCULATED CENTRAL SPECTRA AND ADJOINTS
CROSS-SECTION SET 192 (RE-122)[12]

Group	Assembly 34		Assembly 42	
	ϕ	ϕ^*	ϕ	ϕ^*
1	0.0186	0.0616	0.0187	0.0629
2	0.0371	0.0610	0.0370	0.0620
3	0.0676	0.0581	0.0671	0.0588
4	0.1041	0.0539	0.1035	0.0542
5	0.1421	0.0549	0.1424	0.0550
6	0.1513	0.0579	0.1521	0.0579
7	0.1297	0.0601	0.1303	0.0601
8	0.0970	0.0622	0.0977	0.0620
9	0.0793	0.0632	0.0796	0.0630
10	0.0685	0.0641	0.0685	0.0638
11	0.0336	0.0656	0.0336	0.0652
12	0.0364	0.0662	0.0359	0.0658
13	0.0181	0.0682	0.0177	0.0677
14	0.00718	0.0684	0.0070	0.0679
15	0.00776	0.0683	0.00748	0.0678
16	0.00149	0.0664	0.00142	0.0660

NUCLEAR TRACK EMULSION EXPOSURES

Several irradiation runs were made in which 400-μ-thick Ilford E-1, 100-μ-thick Ilford L-4, and 100-μ-thick Gevaert 307 emulsions were exposed to total integrated fluxes of from 1×10^8 to 6×10^9 nvt. Twenty-one emulsion packets representing seven of each type were sent to Northwestern University for analysis. Nine mixture Ilford L-4 cadmium-covered emulsion packets were sent to Centre d'Etudes de L'Energie Nucleaire, Mol-Donk, Belgium.

FISSION RATE AND REACTION RATE TRAVERSES

Relative fission rates of various fissile isotopes and reaction rates of boron-10 have been measured along radii extending through the core center and also along the core axial midline. The relative fission rates of U^{235}, U^{234}, U^{238}, and Pu^{239}, as well as the reaction rate of B^{10} as measured by an enriched BF_3 counter, were measured both axially and radially.

The radial measurements were made by traversing miniature cylindrical counters through a guide tube radially from the top of the core down through the core center. A vertical guide tube is recessed into the 16th row of the movable half (Half No. 2) by inserting the tube in holes drilled through the tops and bottoms of the matrix tubes in this row. The counters used in this manner are displaced axially approximately $\frac{1}{4}$ in. from the core center. The $\frac{1}{4}$-in. axial displacement does not alter the fission rate results in fast reactors of this size.

Axial measurements were made by modifying two opposing central drawers (1 and 2-O-16) to allow them to accept the $\frac{1}{2}$-in.-diameter guide tube. This guide tube is fixed in position in the movable half (Half No. 2) and is allowed to slide through the center of the stationary half. This allows closure of the halves after the traverse mechanism has been bolted to the movable half and the traverse counter positioned in the movable half end of the guide tube. Both radial and axial flux distribution measurements were made parallel to the fuel plates to assure that fine-structure effects would not disrupt a normally smooth distribution of flux due to variations in counter-fuel proximity. The measured fission rate distributions are given in Figs. 22 through 29, and reaction rate distributions for boron-10 in Figs. 30 and 31.

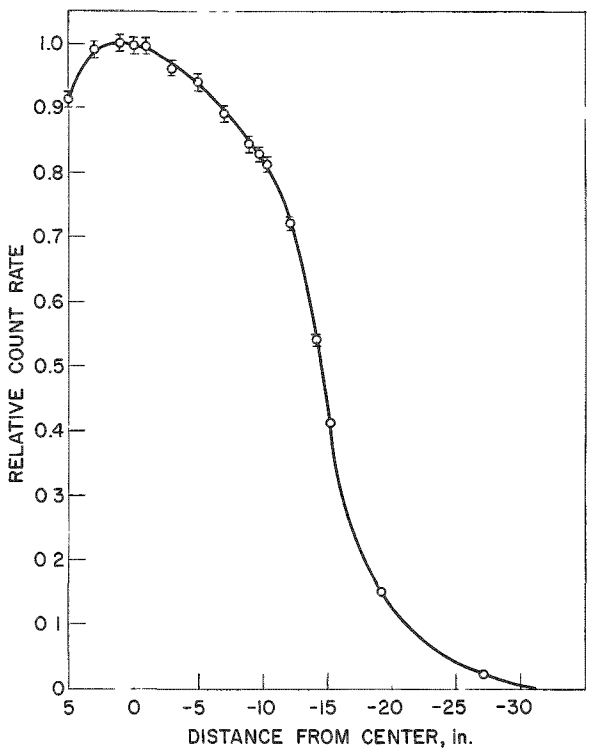

Fig. 22. Radial U^{235} Fission Distribution

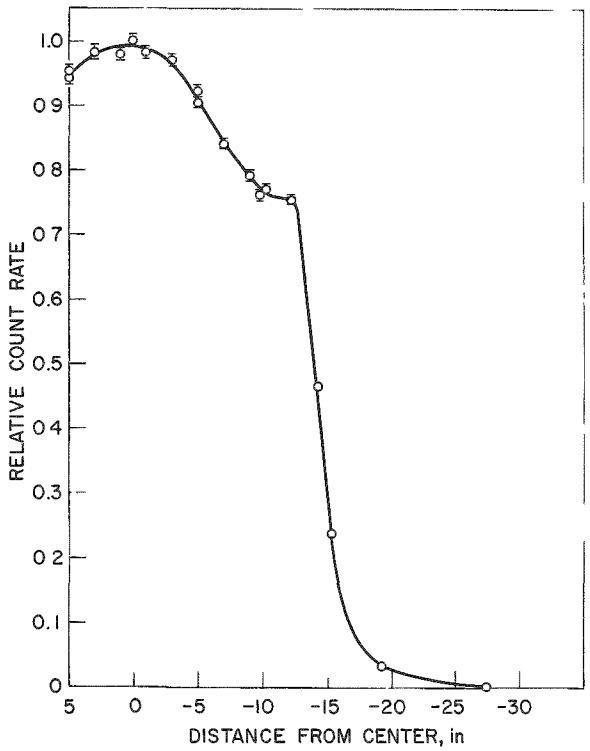

Fig. 23. Radial U^{238} Fission Distribution

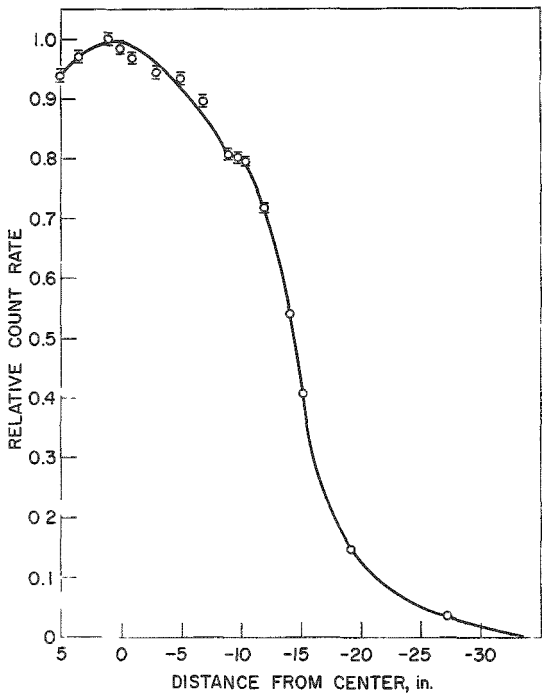

Fig. 24. Radial Pu^{239} Fission Distribution

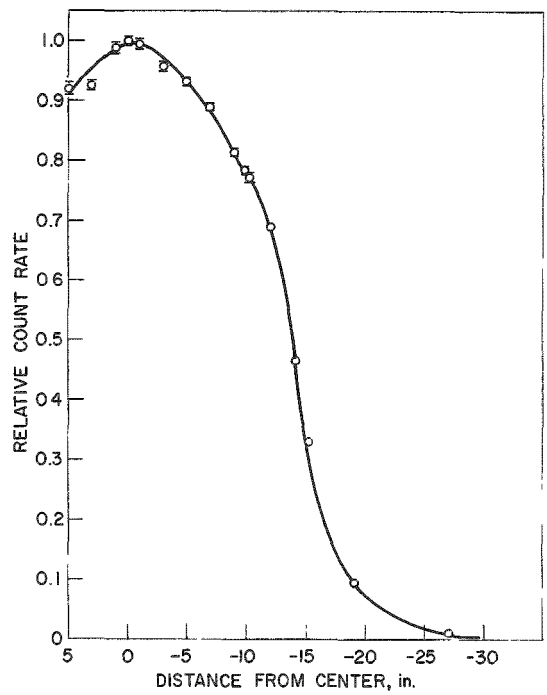

Fig. 25. Radial U^{234} Fission Distribution

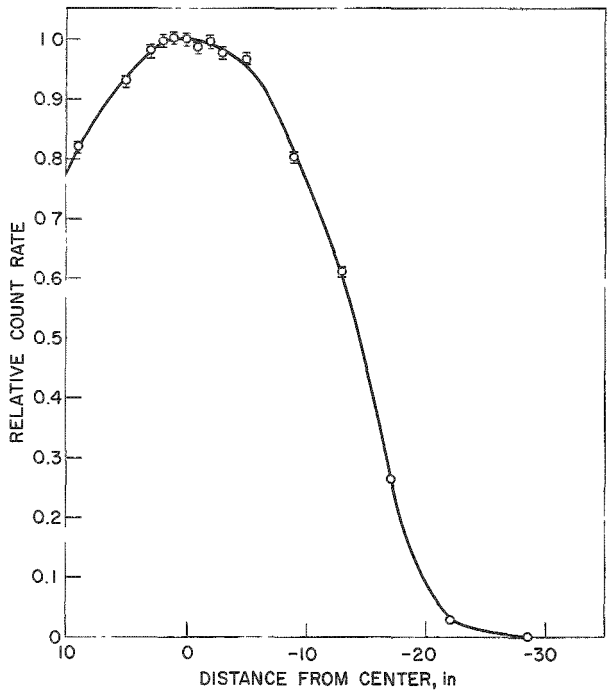

Fig. 26. Axial U^{235} Fission Distribution

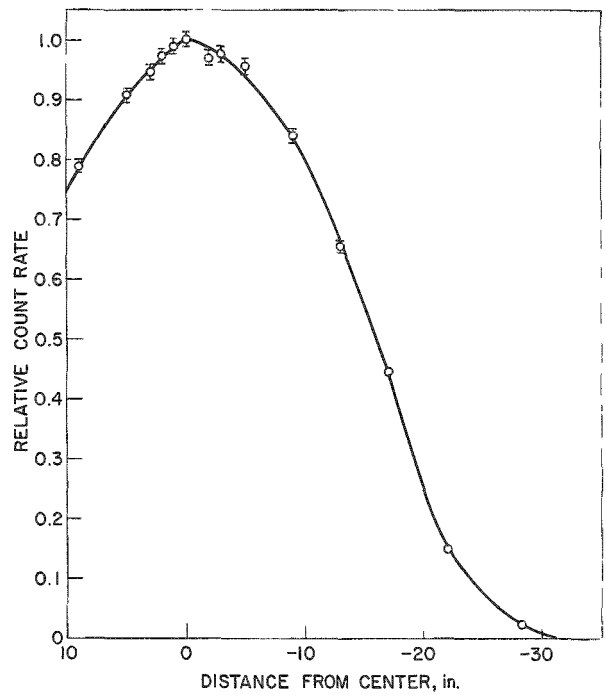

Fig. 27. Axial U^{238} Fission Distribution

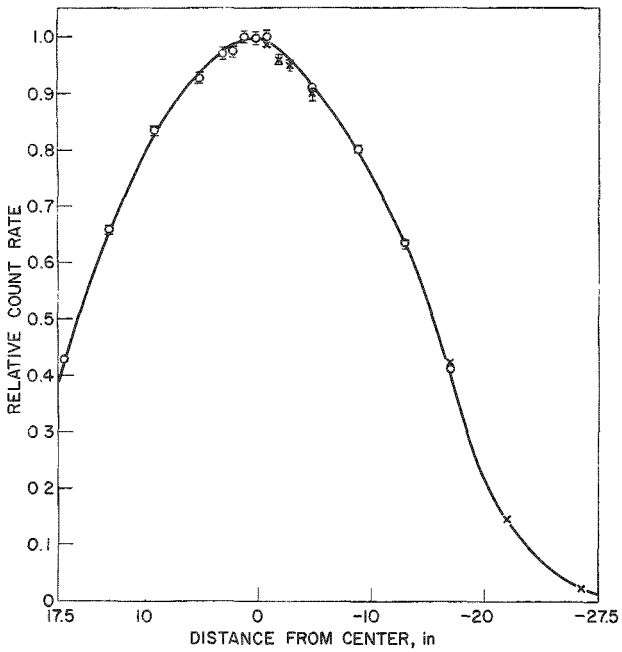

Fig. 28. Axial Pu^{239} Fission Distribution

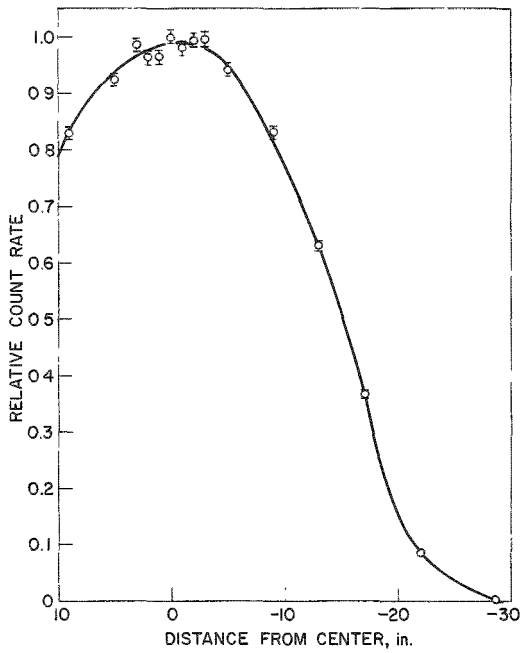

Fig. 29. Axial U^{234} Fission Distribution

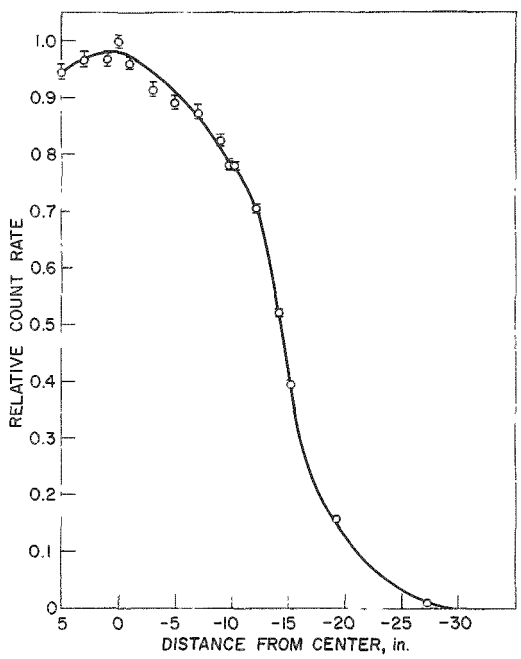

Fig. 30. Radial BF_3 Reaction Rate Distribution

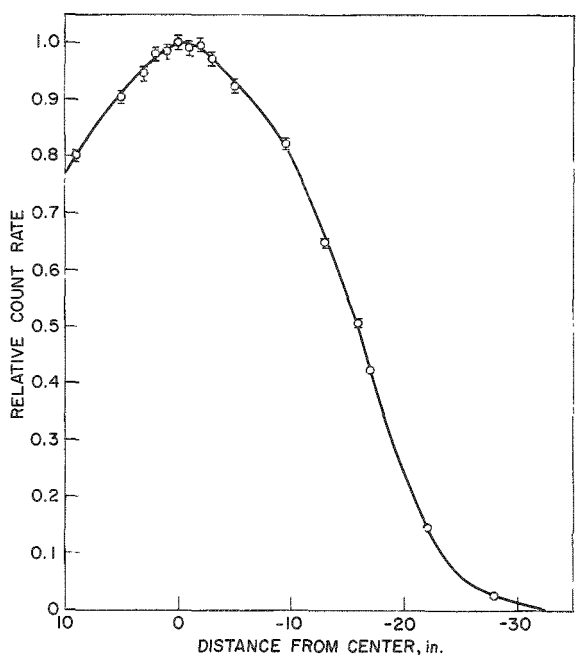

Fig. 31. Axial BF_3 Reaction Rate Distribution

ROSSI-ALPHA MEASUREMENTS

Since this reactor consisted of two zones differing greatly in composition, three different arrangements of four BF_3 counters were used to determine if the different lifetimes of each region can be measured. The results are given in Table VII.

Table VII

ROSSI-ALPHA MEASUREMENTS

	Alpha at delayed critical ($sec^{-1} \times 10^{-4}$)
A. Both initiating and terminating counters at center of core	3.68
B. Initiating counter at center of core - terminating counter in driver region	3.76
C. Reverse of B above	3.67

Since the uncertainty of each measurement is of the order of 2%, there is no credible divergence in the above results.

An interesting computation can be performed in this connection. An average of the above results gives a value of 3.70×10^4 sec^{-1} for alpha at delayed critical. Taking 0.0072 as a reasonable value for $\beta_{effective}$, we obtain a lifetime

$$L = \frac{7.2 \times 10^{-3}}{3.70 \times 10^4} = 19.5 \times 10^{-8} \text{ sec.}$$

However, if we ignore all the experimental results with this assembly, we can estimate the lifetime by use of the empirical methods of Brunson et al.[14] From fission rate profiles for U^{235} and U^{238} (see Figs. 22 and 23), it is estimated that the relative importance of the two regions is 1:1. This takes into account the fact that 140 kg of fuel in the central region sees a higher flux and occupies a position of greater importance than the 240 kg of U^{235} in the driver region.

From previous results the lifetime for Assembly 34 core composition is 24.7×10^{-8} sec. We can with somewhat less assurance estimate the characteristic lifetime in the driver composition. We note from Yiftah, et al.[7] that Assembly 12 with ~37 v/o graphite has a lifetime 14% greater than the predicted lifetime of an all-metal assembly having the same V* (see below). Assembly 17 with ~53 v/o graphite has a lifetime 30% greater than a corresponding all-metal system. The driver region has ~47 v/o graphite, and

we obtain by hopeful interpolation an estimate that the lifetime of this composition will fall 25% above that of an all-metal assembly of the same V*. The V* here is 0.089, for which we reach an all-metal lifetime of 11.8×10^{-8} sec. Applying the 25% correction estimated above, we obtain a lifetime of 14.7×10^{-8} sec.

If we average these two lifetimes on a 1:1 basis as discussed above, we obtain

$$\frac{(24.7 + 14.7)}{2} \; 10^{-8} = 19.7 \times 10^{-8} \text{ sec.}$$

In the above discussion the term V* is taken as the volume fraction of U^{235} plus $\frac{1}{9}$ the volume fraction of U^{238}.

FOIL IRRADIATIONS

Natural and enriched uranium foils were irradiated at points along the radial and axial midlines of the assembly.

All the foils were irradiated during a 50 Whr run. The natural uranium foils were all positioned in the stationary half (Half No. 1) and the enriched foils in the movable half (Half No. 2).

The foils irradiated along the cylindrical axis were positioned between sections of fuel in drawers 1 and 2-O-16 as shown in Fig. 32. The irradiations along the radial midline were performed by placing foils at the front and top of two drawers in the core and one in the driver. A view of the foil positions for these drawers is given in Fig. 33.

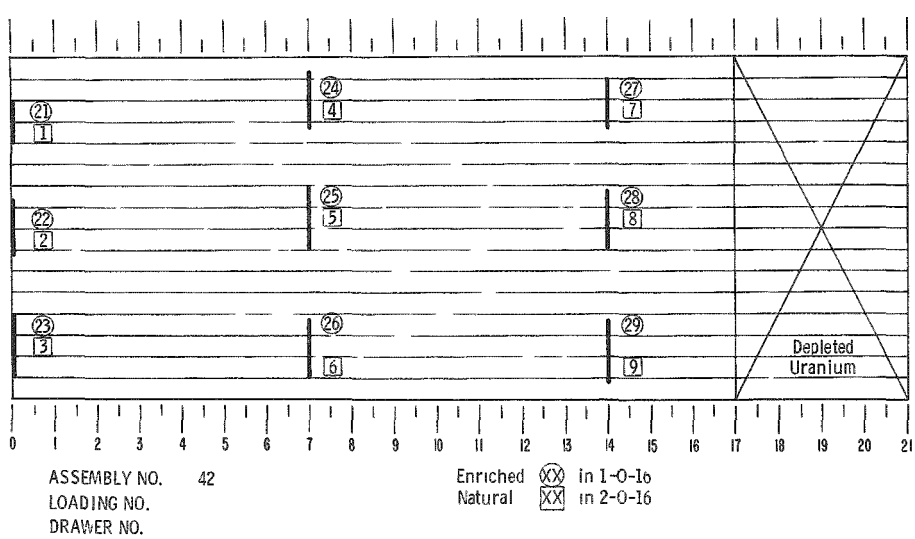

Fig. 32. Foil Irradiation Positions (Axial)

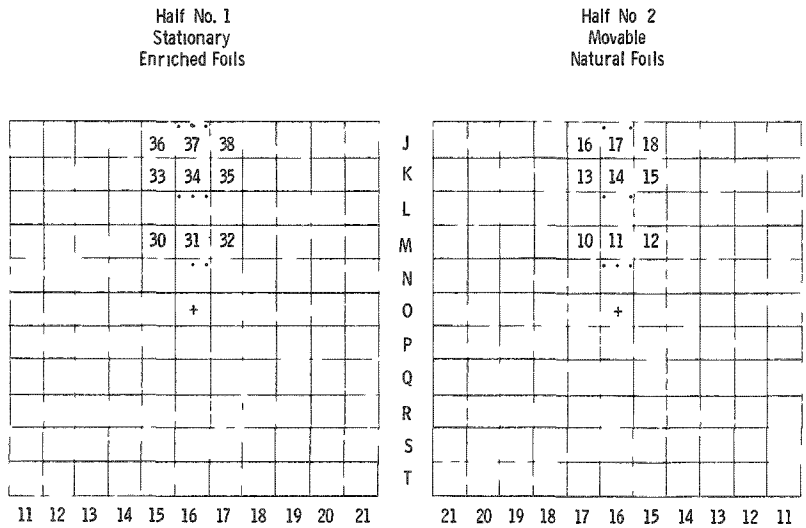

Fig. 33. Foil Irradiation Positions (Radial)

In all cases the foils were wrapped in a double thickness of aluminum foil.

The radiochemical analysis of the foils was performed at Argonne, Illinois. The U^{238}:U^{235} fission and capture ratios were determined from the total induced activity of Mo^{99} and Np^{239} respectively. A tabulation of the experimental results is given in Table VIII.

Table VIII

FISSION AND CAPTURE ANALYSIS OF DEPLETED AND ENRICHED URANIUM FOILS

Group No.	Foil No.	Total Mass (g)	Total Fissions	Fissions, g	Total Captures	Captures, g
1-N	1-2-3	11.6298	8.93×10^{9}	7.67×10^{8}	2.21×10^{10}	1.90×10^{9}
2-N	4-5-6	11.4191	8.02×10^{9}	7.02×10^{8}	2.00×10^{10}	1.75×10^{9}
3-N	7-8-9	11.8190	5.33×10^{9}	4.51×10^{8}	1.42×10^{10}	1.20×10^{9}
4-N	10-11-12	11.3080	8.24×10^{9}	7.29×10^{8}	2.19×10^{10}	1.94×10^{9}
5-N	13-14-15	11.4338	7.39×10^{9}	6.46×10^{8}	2.06×10^{10}	1.80×10^{9}
6-N	16-17-18	11.7325	7.06×10^{9}	6.02×10^{8}	1.71×10^{10}	1.46×10^{9}
1-E	21-22-23	1.0790	1.85×10^{10}	1.72×10^{10}		
2-E	24-25-26	1.0750	1.56×10^{10}	1.45×10^{10}		
3-E	27-28-29	1.1273	1.17×10^{10}	1.04×10^{10}		
4-E	30-31-32	1.0613	1.79×10^{10}	1.68×10^{10}		
5-E	33-34-35	1.1132	1.67×10^{10}	1.50×10^{10}		
6-E	36-37-38	1.1239	1.37×10^{10}	1.22×10^{10}		

The foils were analyzed in groups of three to get an average over the drawer for any one position and also to increase the activity for better statistics. In all cases the errors are taken to be ±3%.

The fission and capture ratios calculated from this experimental data are given in Table IX.

Table IX

ENRICHED AND NATURAL URANIUM FOIL IRRADIATIONS

Distance from Core Center (cm)		Fissions/g U^{238}	Captures/g U^{238}	Fissions/g U^{235}	$\frac{\bar{\sigma}_f\ U^{238}}{\bar{\sigma}_f\ U^{235}}$	$\frac{\bar{\sigma}_c\ U^{238}}{\bar{\sigma}_f\ U^{235}}$
Axial	Radial					
0	2.5	6.39×10^8	1.91×10^9	1.85×10^{10}	0.035	0.103
17.8	2.5	5.95×10^8	1.76×10^9	1.56×10^{10}	0.038	0.113
35.6	2.5	3.79×10^8	1.21×10^9	1.12×10^{10}	0.034	0.108
0.6	8.3	6.13×10^8	1.95×10^9	1.80×10^{10}	0.034	0.108
0.6	18.8	5.43×10^8	1.81×10^9	1.61×10^{10}	0.034	0.112
0.6	29.8	5.18×10^8	1.47×10^9	1.31×10^{10}	0.039	0.112

SODIUM IRRADIATIONS

The increasing trend toward larger (500-4000 liters) fast reactor cores has spurred interest in low-energy spectral indices.

This experiment attempts to utilize the (n, γ) reaction in the 2.85-keV sodium resonance. This measurement is useful in large systems containing materials that have no interfering resonances and whose energy spectra is such that the resonance reaction is a constant fraction of the total sodium activation, and where the sample resonant flux depression is small enough so as not to change the percentage of activation due to resonant absorption over the range of reactor spectra that are studied.

One-dimensional diffusion-theory calculations (RE-122)[15] indicate that the (n, γ) reaction in the 2.85-keV sodium resonance accounts for 86.6 ± 1% of the total sodium activations at any point in the core or driver.

Sodium was irradiated in the form of sodium nitrate powder contained in $\frac{3}{8}$-in.-dia by 2-in.-long aluminum capsules. The capsules were placed in $\frac{3}{8}$-in.-thick voids created at various positions in the reactor. The natural and enriched uranium foils were irradiated (see Table IX) in symmetrical positions during the same run.

The sodium nitrate powder was then dumped into a $1\frac{1}{2}$ dram bottle and washed. The bottle was then filled with water to a predetermined height and was placed in a scintillation well counter. An integral count of all gamma rays above 1 MeV was taken.

The ratio of the absolute β disintegration rate to the observed γ count rate of the calibration sample was used to determine the absolute decay rate of the irradiated samples. To account for the radial flux shape the measured sodium activity was divided by the U^{235} fission rate (see Table X).

Table X

SODIUM ACTIVATION MEASUREMENTS

Sample	Location	Radius, cm	$\frac{\text{Counts/m}}{\text{g } NaNO_3}$	$\frac{\bar{\sigma}_a\ (Na)}{\bar{\sigma}_f\ (U^{235})}$ (normalized to unity at core center)
1D	1 O 16	0	4313	1.0
2D	1 M 16	11.2	4311	1.057
3D	1 K 16	22.1	3934	1.066
5D	1 I 16	33.3	3285	1.18
8D	1 G 16	44.2	1018	1.06
7D	1 G 17	44.7	748	0.804

A plot of the normalized (unity at core center) calculated[15] and experimental ratios is given in Fig. 34.

An absolute calibration was performed by counting a calibration sample of activated sodium nitrate solution. The absolute activity of the calibration sample was determined by a 4π β counter and a 4π liquid scintillator.

A preliminary absolute calibration yielded a value of $\bar{\sigma}_a\ (Na)/\bar{\sigma}_f\ (U^{235}) = 0.70 \times 10^{-3} \pm 8\%$.

Preliminary calculations indicate that the resonant flux depression for the sample size used may be as large as 40%. An experiment to determine flux depression vs. sample size will clarify this point for future sodium irradiations.

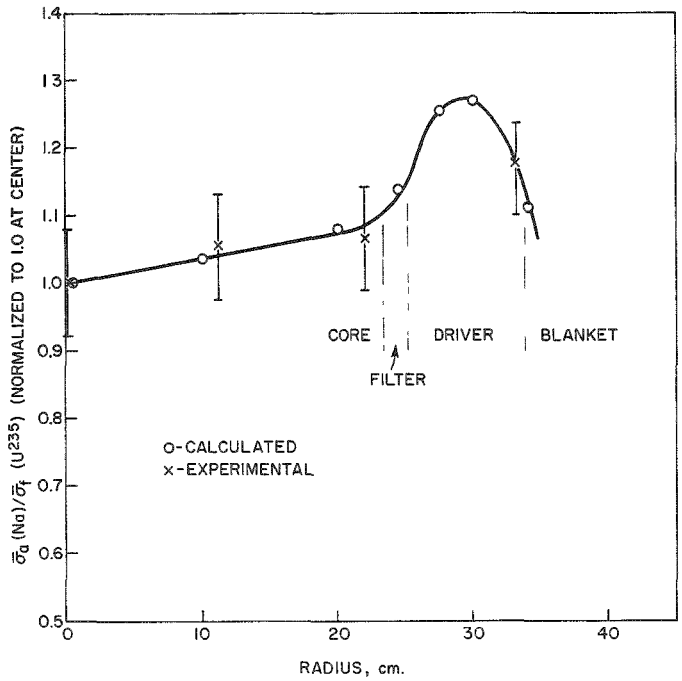

Fig. 34. Radial $\frac{\bar{\sigma}_a\ (\mathrm{Na})}{\bar{\sigma}_f\ (U^{235})}$ Distribution

REFERENCES

1. Huber, R. J. et al., Critical Studies of a Dilute Carbide Fast Reactor Core, (ZPR-III Assembly 34), ANL-6401 (1961).
2. Cerutti, B. C. et al., ZPR-III, Argonne's Fast Critical Facility, Nuclear Science and Engineering, 1, 126 (1956).
3. Keeney, W. P. et al., Dilute Fast Critical Experiments in Zero Power Reactor Number III, Trans. ANS., 3, 327 (1960).
4. Meneghetti, D. et al., Calculation of Heterogeneity Effects in ZPR-III Fast Assemblies Using the DSN Program, ANL-6218 (1960).
5. Davey, W. G., k Calculations for 22 ZPR-III Fast Reactor Assemblies Using ANL Cross-Section Set 635, ANL-6570 (1962).
6. Davey, W. G., A Comparison of Experimental and Calculated Prompt Neutron Lifetimes and Central Reactivity Coefficients in ZPR-III Assemblies and Their Relationship to Other Reactor Parameters, ANL-6682 (1962).
7. Yiftah, S. et al., Fast Reactor Cross Sections, Pergamon Press (1960).
8. Long, J. K. et al., Fast Neutron Power Reactor Studies with ZPR-III, Second UN Intnl. Conf. on Peaceful Uses of Atomic Energy, Geneva, Switzerland, 12, 119 (1958).
9. Amundson, P. I , Critical Studies of Uranium-Steel and Uranium-Steel-Sodium Fast Reactor Cores (ZPR-III Assemblies 32 and 33), ANL-6690 (Feb 1963).
10. Kirn, F. S., An Absolute Fission Counter, American Nuclear Society, 2nd Winter Meeting (1957).
11. Davey, W. G., A Critical Comparison of Measured and Calculated Fission Ratios for ZPR-III Assemblies, ANL-6617 (1962).
12. McVean, R. L. et al., The Role of the Fast Critical Facility in the Power Reactor Program, Proc. of the Symposium on Exponential and Critical Experiments; International Atomic Energy Agency, Amsterdam, Sept, 1963.
13. Davey, W. G. et al., An Experimental Investigation of Some Sources of Error in the Measurement of Absolute Fission Ratios in Fast Reactors, ANL-6468 (1961).
14. Brunson, G. S. et al., Measuring the Prompt Period of a Reactor, Nucleonics, 15, 132 (1957).
15. Fischer, George J., Private communications.